JHWCR JOURNAL OF HEALTH, WELLNESS AND COMMUNITY RESEARCH 3007-0570

DOI: https://doi.org/10.61919/4t879b92

Original Article

Nano-Encapsulation of Herbal Alkaloids for Targeted Anti-Cancer Delivery

Aatqa Rauf[1], Zahoor Islam[2], Fazal Hadi[3], Hajra Afeera Hamid[4], Afshan Pervaiz[5], Muhammad Azhar Sherkheli[6]

[1] Lecturer, Federal Urdu University of Arts, Sciences and Technology, Islamabad, Pakistan
[2] Visiting Lecturer, Riphah International University, Malakand Campus, Malakand, Pakistan
[3] PhD Scholar, Abdul Wali Khan University Mardan, Mardan, Pakistan
[4] Assistant Professor, Allied Health Sciences, University of Science and Technology Bannu, Bannu, Pakistan
[5] PhD Bioscience, Mohammad Ali Jinnah University, Karachi, Pakistan
[6] Professor, Department of Pharmacy, Abbottabad University of Science and Technology, Abbottabad, Pakistan

***Corresponding author: Muhammad Azhar Sherkheli, azhar.sherkheli@gmail.com**

"Cite this Article" Received: 09 February 2026; **Accepted**: 20 March 2026; **Published**: 30 March 2026

Author Contributions: Concept: AR, MAS; Design: ZI, FH, MAS; Data Collection: AR, HAH, AP; Analysis: ZI, FH; Drafting: AR, HAH, AP, MAS. **Ethical Approval**: Bahria University Pharmacology Lab, Islamabad, Pakistan. **Informed Consent**: Written informed consent was obtained from all participants; **Conflict of Interest**: The authors declare no conflict of interest. **Funding**: No external funding; **Data Availability**: Available from the corresponding author on reasonable request; **Acknowledgments**: NA

ABSTRACT

Background: Herbal alkaloids have potential cytotoxic activity but may be limited by poor solubility, restricted bioavailability, and rapid release. Objective: To prepare and characterize PLGA–chitosan nanoparticles containing berberine and piperine and compare the release and MCF-7 cytotoxicity of free and nanoencapsulated berberine. Methods: In this in vitro experimental study, blank, berberine-loaded, piperine-loaded, and combined berberine–piperine nanoparticles were prepared by modified solvent evaporation. Particle size, polydispersity index, zeta potential, encapsulation efficiency, and drug loading were evaluated. Berberine release was assessed for up to 48 hours, and MCF-7 metabolic viability was measured by MTT assay after 48-hour exposure. Results: Berberine-loaded nanoparticles had a particle size of 156.8 ± 5.6 nm, zeta potential of +24.7 ± 2.1 mV, encapsulation efficiency of 82.6 ± 3.4%, and drug loading of 14.8 ± 1.2%. At 4 and 24 hours, cumulative release was 34.5% and 76.4% from nanoparticles compared with 66.8% and >94% from free berberine. At 100 µg/mL, MCF-7 viability was 21.5 ± 2.8% with nanoencapsulated berberine and 39.7 ± 3.6% with free berberine. The reported IC_{50} values were 38.7 and 56.4 µg/mL, respectively. Conclusion: Nanoencapsulation modified berberine release and was associated with lower MCF-7 metabolic viability under the tested in vitro conditions. Verification of the source data and further selectivity, mechanistic, and preclinical studies are required. Keywords: Berberine; Piperine; PLGA Nanoparticles; Chitosan; Drug Release; MCF-7 Cells; Cytotoxicity; Nanoencapsulation.

INTRODUCTION

Cancer remains a major cause of morbidity and mortality worldwide, with approximately 19.3 million new cases and 10 million cancer-related deaths estimated in 2020. Its burden continues to increase because of population growth, ageing, environmental exposures, lifestyle-related risk factors, oncogenic infections, and disparities in prevention, early detection, and treatment access (1,2). Pakistan also carries a substantial cancer burden. National and regional registry data have identified breast cancer as the most frequently reported malignancy among women, while registries from Lahore and Karachi have demonstrated considerable geographic and sex-related variation in cancer incidence (3–6). These patterns emphasize the need for therapeutic strategies that improve drug delivery while reducing exposure of non-target tissues.

Conventional anticancer agents may be limited by systemic toxicity, inadequate tumor penetration, poor aqueous solubility, chemical instability, rapid elimination, and the development of cellular drug resistance. These limitations can reduce the amount of therapeutically active compound reaching malignant tissue and may necessitate higher or repeated doses, thereby increasing treatment-related

adverse effects. Drug-delivery systems capable of improving solubility, protecting active molecules from premature degradation, prolonging drug release, and enhancing intracellular exposure have therefore become an important focus of cancer pharmacology (7,8).

Nanoparticle-based carriers provide one approach to modifying the pharmacokinetic and physicochemical behavior of anticancer compounds. Polymeric nanoparticles can incorporate poorly soluble drugs within a biodegradable matrix, protect them from environmental degradation, and regulate their release over time. Their biological performance depends on several interrelated characteristics, including particle size, size distribution, surface charge, composition, morphology, drug-loading capacity, and interactions with plasma proteins and cellular membranes (9–11). Although nanoparticles may exhibit preferential accumulation in some tumors through abnormalities in tumor vasculature, the magnitude and reproducibility of this phenomenon vary considerably across tumor types and experimental models. Consequently, particle size and surface characteristics alone cannot establish tumor targeting, and formulation studies must distinguish physicochemical suitability from experimentally demonstrated biological selectivity (9,10).

Poly(lactic-co-glycolic acid) is a biodegradable and biocompatible polymer widely investigated for controlled drug delivery. PLGA nanoparticles can encapsulate hydrophobic or poorly bioavailable compounds and provide sustained release through diffusion and polymer degradation. Chitosan may be incorporated as a surface-modifying polymer because its cationic properties can alter nanoparticle charge, dispersibility, and interaction with negatively charged biological membranes. Nevertheless, the biological benefits of these characteristics must be established experimentally rather than inferred solely from physicochemical measurements (12–15).

Natural alkaloids represent a chemically diverse group of nitrogen-containing plant constituents with potential pharmacological activity against cancer-related pathways. Several alkaloids have been reported to influence cellular proliferation, apoptosis, oxidative stress, inflammation, migration, and cell-cycle regulation. However, their pharmaceutical development is frequently constrained by poor aqueous solubility, limited absorption, rapid metabolism, low systemic bioavailability, and dose-dependent toxicity. Nanoencapsulation has therefore been investigated as a method for improving the delivery of natural bioactive compounds without assuming that such compounds can replace established anticancer treatment (16,17).

Berberine is an isoquinoline alkaloid obtained from medicinal plants including species of Berberis. Experimental evidence suggests that berberine may affect apoptosis, cell-cycle progression, inflammatory signaling, oxidative balance, and pathways involved in breast, lung, and hepatic malignancies (18,19). Its therapeutic application is nevertheless restricted by poor gastrointestinal absorption and low bioavailability. Berberine has consequently been incorporated into several delivery platforms, including PLGA nanoparticles, gold nanoparticles, liquid-crystalline nanoparticles, microfluidically produced nanoparticles, and hyaluronic acid-modified polymeric systems. These formulations have shown improved drug incorporation, sustained release, cellular exposure, or cytotoxic activity in selected preclinical models (20–25).

Piperine, the principal pungent alkaloid of black pepper, has also demonstrated cytotoxic and chemosensitizing properties in experimental cancer models. Polymeric piperine nanoparticles have been evaluated in breast cancer cell systems, with some studies reporting improved physicochemical performance and greater reductions in cellular viability than free piperine (26,27). However, formulation characteristics and biological responses vary with polymer composition, drug-to-polymer ratio, surface modification, exposure concentration, assay conditions, and cell-line characteristics. Direct evaluation of each formulation is therefore necessary.

Despite growing evidence regarding alkaloid-based nanocarriers, several uncertainties remain concerning the relationship between formulation characteristics, release behavior, and in vitro

cytotoxicity. In particular, comparative characterization of berberine- and piperine-containing polymeric nanoparticles may clarify whether these compounds can be incorporated efficiently into PLGA–chitosan systems and whether nanoencapsulation modifies their release and observed effects on breast cancer cell viability. Such experiments represent an early formulation-development stage and do not independently demonstrate tumor targeting, clinical efficacy, or safety.

The present experimental pharmacological study was therefore conducted to prepare and characterize PLGA–chitosan nanoparticles containing berberine, piperine, or both alkaloids and to assess their particle size, polydispersity index, zeta potential, encapsulation efficiency, drug loading, morphology, and in vitro release behavior. The study further compared the effect of free alkaloid, blank nanoparticles, and alkaloid-loaded nanoparticles on the metabolic viability of MCF-7 breast cancer cells using the MTT assay. It was hypothesized that nanoencapsulation would produce a more controlled release profile and a greater concentration-dependent reduction in MCF-7 cell viability than the corresponding free alkaloid under the tested in vitro conditions.

MATERIALS AND METHODS

This in vitro experimental pharmacological study was conducted in a controlled research laboratory in Islamabad, Pakistan. The investigation comprised nanoparticle formulation, physicochemical characterization, in vitro drug-release evaluation, and cell-based cytotoxicity testing. Berberine and piperine were selected as model herbal alkaloids because of their reported anticancer properties and pharmaceutical limitations, including low aqueous solubility and restricted bioavailability (18,19,26,27). Poly(lactic-co-glycolic acid) was used as the principal biodegradable polymer, while chitosan was incorporated to modify the surface characteristics of selected formulations. Polyvinyl alcohol was used as a stabilizing agent. Other laboratory materials included organic solvent, ethanol, phosphate-buffered medium, dimethyl sulfoxide, cell-culture medium, fetal bovine serum, antibiotics, trypsin, MTT reagent, and analytical-grade reagents required for formulation preparation, drug quantification, and cell-culture procedures.

Berberine-loaded, piperine-loaded, combined berberine–piperine, and drug-free blank nanoparticles were prepared using a modified solvent-evaporation technique. The selected alkaloid and PLGA were dissolved in an organic phase, which was introduced gradually into an aqueous phase containing the stabilizing agent under continuous mixing. Chitosan was incorporated into the relevant formulations to produce positively charged surface-modified nanoparticles. The resulting dispersion was processed to promote the formation of nanosized particles, after which the organic solvent was removed under controlled conditions. Nanoparticles were subsequently separated by centrifugation, washed to remove unencapsulated alkaloid and residual stabilizer, dried, and stored in closed containers until characterization. Blank nanoparticles were prepared using the same procedure without incorporating berberine or piperine and were used to evaluate carrier-related effects.

Multiple formulation batches were produced by varying the relative concentrations of the polymer, alkaloid, and stabilizing components. Candidate formulations were compared according to particle size, polydispersity index, zeta potential, encapsulation efficiency, drug loading, dispersibility, and release behavior. The formulation showing the most appropriate combination of nanoscale particle size, acceptable size uniformity, positive surface charge, efficient drug incorporation, and sustained release was selected for subsequent release and cytotoxicity evaluation. The optimization process was based on the collective physicochemical performance of the prepared formulations rather than particle size alone.

The physical appearance, color, sedimentation, aggregation, and redispersibility of freshly prepared nanoparticle suspensions were examined visually. Mean hydrodynamic particle size, polydispersity index, and zeta potential were measured by dynamic light scattering. Particle size was used to characterize the nanoscale dimensions of the formulation, while the polydispersity index was used to assess the uniformity of the particle-size distribution. Zeta potential was measured to estimate the surface

charge and colloidal behavior of the formulations. Measurements were performed on appropriately dispersed samples, and replicate readings were summarized as mean and standard deviation.

Encapsulation efficiency and drug loading were determined after separating unencapsulated alkaloid from the nanoparticle fraction. The concentration of free or extracted alkaloid was quantified using the analytical procedure employed for the study. Encapsulation efficiency was calculated as the proportion of the initially added alkaloid retained within the recovered nanoparticles, whereas drug loading was calculated as the mass of incorporated alkaloid relative to the mass of the recovered drug-loaded formulation. Separate measurements were required for berberine and piperine in the combined formulation to distinguish the incorporation efficiency of each compound.

The morphology of the optimized nanoparticles was examined by scanning electron microscopy. Dried nanoparticle samples were mounted on a suitable specimen holder and prepared for microscopic visualization. The micrographs were assessed for particle shape, surface appearance, aggregation, and agreement between the observed morphology and the hydrodynamic measurements obtained by dynamic light scattering. Morphological assessment was treated as complementary to, rather than a replacement for, quantitative particle-size analysis.

In vitro drug release was evaluated in phosphate-buffered medium under physiologically relevant pH conditions. Free alkaloid and drug-loaded nanoparticles containing an equivalent nominal amount of alkaloid were evaluated separately. The formulations were placed in the release medium under continuous controlled agitation, and aliquots were collected at predetermined intervals over a 48-hour period. An equivalent volume of fresh medium was added following each collection to maintain the release volume and support sink conditions. The concentration of released alkaloid was quantified using the same validated analytical approach used for drug determination, and cumulative release was expressed as a percentage of the initially incorporated or available alkaloid after correction for serial sampling.

Release profiles were assessed using zero-order, first-order, Higuchi, and Korsmeyer–Peppas kinetic models. The zero-order and first-order models were used to evaluate concentration-independent and concentration-dependent release patterns, respectively, whereas the Higuchi model was used to assess diffusion-related release from the polymeric matrix. The Korsmeyer–Peppas model was used to explore the contribution of diffusion and polymer-associated transport mechanisms to drug release (34,35). Model selection was based on the goodness of fit of the observed release data and the estimated model parameters.

The cytotoxicity experiment was conducted using MCF-7 human breast adenocarcinoma cells. Cells were maintained in an appropriate culture medium supplemented with fetal bovine serum and antibiotics and were incubated under standard humidified cell-culture conditions. Cells were subcultured using trypsin and seeded into multiwell culture plates at a density suitable for the MTT assay. Following attachment, the cells were exposed for 48 hours to increasing drug-equivalent concentrations of free alkaloid, alkaloid-loaded nanoparticles, or the corresponding mass of blank nanoparticles. Untreated cells served as the viability control. The same solvent concentration used to prepare the free alkaloid treatment was maintained in the relevant control condition to minimize vehicle-related bias.

Cellular metabolic viability was measured using the MTT colorimetric assay, which is based on the reduction of tetrazolium salt to insoluble formazan by metabolically active cells (36). After the treatment period, MTT reagent was added to each well and incubated to permit formazan formation. The resulting crystals were dissolved in a suitable solvent, and absorbance was measured using a microplate reader. Background absorbance from cell-free wells containing medium, test formulations, or nanoparticles was considered when calculating corrected values because nanoparticle dispersions may interfere with

optical measurements. Cell viability was expressed as a percentage of the untreated or vehicle-matched control, and growth inhibition was calculated from the corresponding viability value.

The half-maximal inhibitory concentration was defined as the drug-equivalent concentration associated with a 50% reduction in metabolic viability relative to the control. IC_{50} values were estimated from the concentration–response relationship for free and nanoencapsulated alkaloid formulations. Blank nanoparticles were evaluated at corresponding carrier concentrations to distinguish alkaloid-associated effects from toxicity attributable to the polymeric vehicle. Because the experiment used only a malignant cell line, the findings were interpreted as comparative cytotoxicity in MCF-7 cells rather than evidence of selective toxicity toward cancer cells or safety in normal tissues.

Experimental measurements were conducted in replicate, and quantitative data were summarized as mean ± standard deviation. Physicochemical characteristics of the formulations were compared using one-way analysis of variance where the assumptions of the test were satisfied. Concentration-dependent cytotoxicity data were evaluated according to treatment group and exposure concentration, while release data were assessed across formulation and sampling time. Pairwise comparisons were undertaken following a significant overall test with adjustment for multiple comparisons. IC_{50} values were estimated using concentration–response modelling. Statistical significance was defined as a two-sided p-value <0.05. Data were analysed using IBM SPSS Statistics version 26.0.

Quality-control measures included preparation of blank nanoparticles, comparison with free alkaloid, use of untreated or vehicle-matched controls, replicate physicochemical measurements, replacement of sampled release medium, and background correction in the MTT assay. Laboratory procedures involving solvents, nanoparticles, and cultured cells were performed in accordance with institutional chemical-safety and biosafety procedures. The investigation did not involve the recruitment of human participants or the direct use of experimental animals; therefore, individual informed consent was not applicable. Institutional authorization for the laboratory work was obtained before commencement of the study.

RESULTS

The nanoparticle formulations were successfully prepared using the modified solvent-evaporation method. Freshly prepared suspensions appeared macroscopically uniform and showed no visible sedimentation. Blank nanoparticles were milky white, berberine-loaded nanoparticles were light yellow, and piperine-loaded nanoparticles had a pale cream appearance. The optimized formulations were readily redispersed following gentle agitation, with no visible large aggregates. Based on the reported particle size, size distribution, surface charge, encapsulation efficiency, and release characteristics, the berberine-loaded PLGA–chitosan formulation was selected for subsequent release and cytotoxicity evaluation.

Table 1. Physicochemical Characteristics of the Nanoparticle Formulations

Formulation	Particle size, nm	Polydispersity index	Zeta potential, mV	Encapsulation efficiency, %	Drug loading, %
Blank nanoparticles	128.6 ± 4.2	0.214 ± 0.030	+21.4 ± 1.8	—	—
Berberine-loaded nanoparticles	156.8 ± 5.6	0.238 ± 0.020	+24.7 ± 2.1	82.6 ± 3.4	14.8 ± 1.2
Piperine-loaded nanoparticles	149.3 ± 6.1	0.251 ± 0.040	+22.9 ± 1.6	78.4 ± 2.9	13.2 ± 1.0
Berberine–piperine-loaded nanoparticles	168.5 ± 7.3	0.269 ± 0.030	+25.6 ± 2.4	80.1 ± 3.1	15.5 ± 1.4

Values are presented as mean ± standard deviation. The number and nature of independent experimental replicates should be confirmed from the original laboratory records. Encapsulation efficiency and drug loading for the combined formulation are reported as presented in the source manuscript; compound-specific values for berberine and piperine were not available.

All formulations had mean particle sizes below 200 nm, ranging from 128.6 ± 4.2 nm for blank nanoparticles to 168.5 ± 7.3 nm for the combined berberine–piperine formulation. The berberine-loaded and piperine-loaded nanoparticles had mean particle sizes of 156.8 ± 5.6 nm and 149.3 ± 6.1 nm,

respectively. Polydispersity index values ranged from 0.214 ± 0.030 to 0.269 ± 0.030, indicating relatively narrow particle-size distributions among the reported formulations.

All nanoparticle formulations showed a positive zeta potential. The highest reported surface charge was observed for the combined berberine–piperine formulation at +25.6 ± 2.4 mV, followed by berberine-loaded nanoparticles at +24.7 ± 2.1 mV, piperine-loaded nanoparticles at +22.9 ± 1.6 mV, and blank nanoparticles at +21.4 ± 1.8 mV. Berberine-loaded nanoparticles had the highest reported encapsulation efficiency among the single-drug formulations at 82.6 ± 3.4%, compared with 78.4 ± 2.9% for piperine-loaded nanoparticles. The corresponding drug-loading values were 14.8 ± 1.2% and 13.2 ± 1.0%, respectively. The combined formulation had the largest particle size and the highest reported total drug loading, although separate encapsulation and loading values for the two alkaloids were not available.

The in vitro release profiles differed descriptively between free berberine and berberine-loaded nanoparticles. Free berberine showed an initial rapid release, reaching 66.8% at 4 hours and more than 94% at 24 hours. By comparison, berberine-loaded nanoparticles released 34.5% of the incorporated drug at 4 hours and 76.4% at 24 hours, followed by continued release through 48 hours. At 4 hours, the cumulative release from the nanoparticle formulation was 32.3 percentage points lower than that of free berberine. At 24 hours, the difference was at least 17.6 percentage points because free berberine release exceeded 94%. These descriptive findings were compatible with an early release phase followed by a slower release phase from the polymeric formulation. Statistical comparison and kinetic-model parameters could not be reported from the available aggregate values.

Table 2. Reported Cumulative In Vitro Release of Free Berberine and Berberine-Loaded Nanoparticles

Formulation	Cumulative release at 4 hours, %	Cumulative release at 24 hours, %	Reported release duration
Free berberine	66.8	>94.0	24 hours
Berberine-loaded nanoparticles	34.5	76.4	48 hours

Complete time-point data, measures of variability, replicate numbers, and kinetic-model coefficients were not available in the source manuscript. These values should be verified against the original release dataset before publication.

The cytotoxicity experiment evaluated untreated control cells, blank nanoparticles, free alkaloid, and alkaloid-loaded nanoparticles over a concentration range of 12.5–100 µg/mL after 48 hours of exposure. The source manuscript did not consistently identify whether the free and nanoencapsulated alkaloid used in this experiment was berberine alone or another tested formulation. Because the optimized berberine-loaded formulation was selected for further testing elsewhere in the manuscript, the treatment is presented below as berberine on that basis; this identity must be confirmed from the original experimental records.

Table 3. MCF-7 Cell Viability After 48-Hour Exposure to Free and Nanoencapsulated Berberine

Treatment group	12.5 µg/mL, %	25 µg/mL, %	50 µg/mL, %	100 µg/mL, %	IC_{50}, µg/mL
Untreated control	100.0 ± 0.0	100.0 ± 0.0	100.0 ± 0.0	100.0 ± 0.0	—
Blank nanoparticles	97.8 ± 2.1	95.6 ± 2.4	93.9 ± 2.7	91.2 ± 3.1	>100
Free berberine	84.6 ± 3.5	70.2 ± 3.8	53.8 ± 4.2	39.7 ± 3.6	56.4
Berberine-loaded nanoparticles	76.3 ± 3.2	58.4 ± 3.6	36.9 ± 3.1	21.5 ± 2.8	38.7

Values are presented as mean ± standard deviation. Concentrations should represent berberine-equivalent exposure and must be confirmed from the original assay records. IC_{50} values are reported as supplied; confidence intervals and nonlinear model-fit statistics were unavailable. The identity of the tested alkaloid must also be verified.

Blank nanoparticles produced only a limited reduction in MCF-7 metabolic viability across the tested concentration range. Mean viability decreased from 97.8 ± 2.1% at 12.5 µg/mL to 91.2 ± 3.1% at 100 µg/mL, corresponding to an absolute reduction of 6.6 percentage points across the tested range. These

findings indicated low observed carrier-associated cytotoxicity under the specific in vitro conditions but did not establish biological safety in normal cells or living organisms.

Both free berberine and berberine-loaded nanoparticles showed concentration-dependent reductions in MCF-7 metabolic viability. At 12.5 μg/mL, viability was 84.6 ± 3.5% following free berberine exposure and 76.3 ± 3.2% following exposure to berberine-loaded nanoparticles, representing an observed between-treatment difference of 8.3 percentage points. At 25 μg/mL, the corresponding values were 70.2 ± 3.8% and 58.4 ± 3.6%, with an observed difference of 11.8 percentage points.

The largest descriptive differences were observed at the two highest concentrations. At 50 μg/mL, cell viability was 53.8 ± 4.2% with free berberine and 36.9 ± 3.1% with berberine-loaded nanoparticles, an absolute difference of 16.9 percentage points. At 100 μg/mL, viability was 39.7 ± 3.6% and 21.5 ± 2.8%, respectively, corresponding to a difference of 18.2 percentage points.

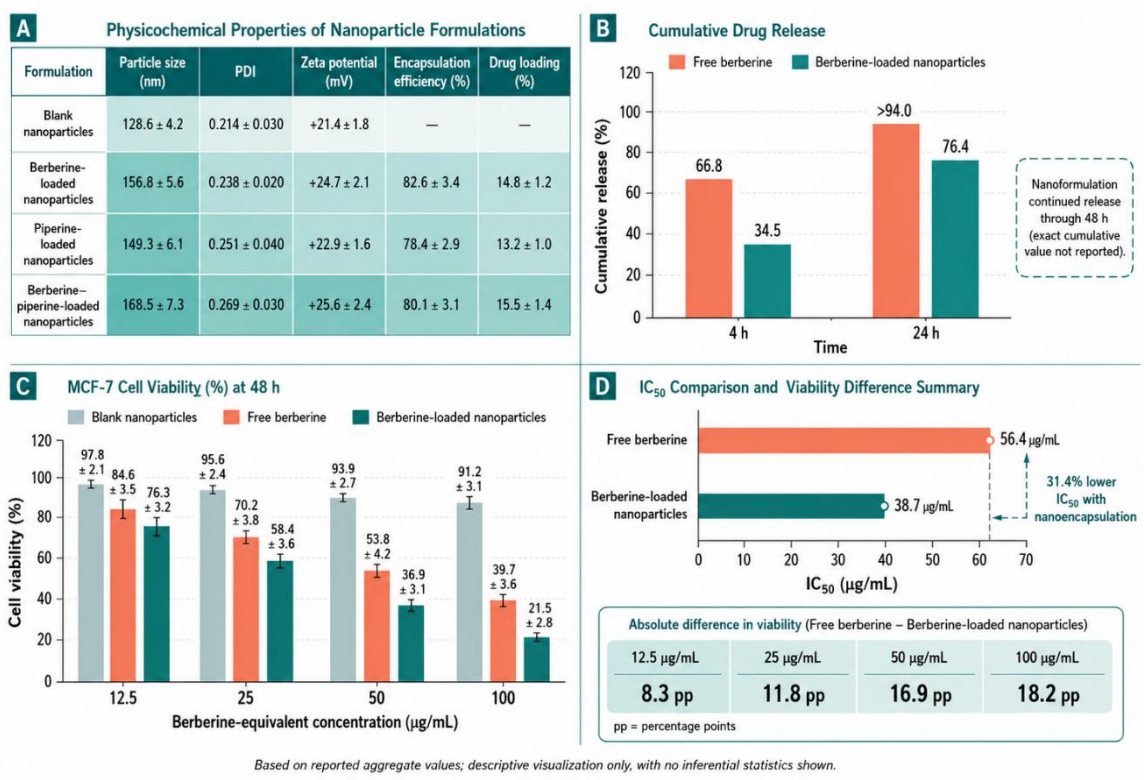

Figure 1. The multipanel figure summarizes the physicochemical characteristics, release behavior, and cytotoxic profile of berberine-loaded PLGA–chitosan nanoparticles. Panel A shows that all formulations had particle sizes below 200 nm, relatively low polydispersity indices, positive zeta potentials, and substantial encapsulation efficiency and drug loading, with berberine-loaded nanoparticles exhibiting a particle size of 156.8 ± 5.6 nm, zeta potential of +24.7 ± 2.1 mV, encapsulation efficiency of 82.6 ± 3.4%, and drug loading of 14.8 ± 1.2%. Panel B demonstrates slower cumulative release from berberine-loaded nanoparticles than from free berberine, with 34.5% versus 66.8% release at 4 hours and 76.4% versus more than 94% at 24 hours, while the nanoformulation continued releasing drug through 48 hours. Panel C shows a concentration-dependent decline in MCF-7 cell viability after 48 hours, with berberine-loaded nanoparticles producing lower viability than free berberine at all tested concentrations; at 100 μg/mL, viability was 21.5 ± 2.8% with the nanoformulation compared with 39.7 ± 3.6% with free berberine, whereas blank nanoparticles maintained viability above 91%. Panel D further shows that the reported IC_{50} decreased from 56.4 μg/mL for free berberine to 38.7 μg/mL for berberine-loaded nanoparticles, representing a 31.4% lower value, while the absolute viability difference between the two treatments increased from 8.3 percentage points at 12.5 μg/mL to 18.2 percentage points at 100 μg/mL.

Table 4. Descriptive Differences in MCF-7 Cell Viability Between Free and Nanoencapsulated Berberine

Berberine-equivalent concentration	Free berberine viability, %	Nanoencapsulated berberine viability, %	Absolute viability difference	Relative reduction versus free berberine, %
12.5 μg/mL	84.6	76.3	8.3	9.8
25 μg/mL	70.2	58.4	11.8	16.8
50 μg/mL	53.8	36.9	16.9	31.4

Berberine-equivalent concentration	Free berberine viability, %	Nanoencapsulated berberine viability, %	Absolute viability difference	Relative reduction versus free berberine, %
100 µg/mL	39.7	21.5	18.2	45.8

Absolute viability difference was calculated as free-berberine viability minus nanoencapsulated-berberine viability. Relative reduction was calculated as the absolute difference divided by free-berberine viability × 100. These are descriptive derived values and do not represent adjusted or statistically tested effects.

The relative reduction in viability associated with nanoencapsulation, compared with free berberine at the same nominal concentration, increased from 9.8% at 12.5 µg/mL to 45.8% at 100 µg/mL. Across the full concentration range, viability declined by 44.9 percentage points in the free-berberine group, from 84.6% to 39.7%, and by 54.8 percentage points in the nanoencapsulated-berberine group, from 76.3% to 21.5%.

The reported IC_{50} was 56.4 µg/mL for free berberine and 38.7 µg/mL for berberine-loaded nanoparticles. The absolute difference between the point estimates was 17.7 µg/mL, while the nanoencapsulated formulation had a reported IC_{50} approximately 31.4% lower than that of free berberine. Because confidence intervals, dose–response model parameters, goodness-of-fit statistics, and independent experimental replicate data were not available, the precision and statistical significance of this difference could not be determined.

Overall, the reported aggregate findings indicated that the prepared nanoparticles had nanoscale dimensions, positive surface charge, and substantial alkaloid incorporation. Berberine-loaded nanoparticles showed slower cumulative drug release than free berberine and lower observed MCF-7 metabolic viability across all tested concentrations. These findings should be interpreted as descriptive in vitro observations. They do not independently demonstrate tumor targeting, selective toxicity toward malignant cells, mechanistic cellular uptake, in vivo safety, or therapeutic efficacy.

DISCUSSION

The present in vitro experimental study evaluated the physicochemical characteristics, drug-release behavior, and MCF-7 cytotoxicity of herbal alkaloids incorporated into PLGA–chitosan nanoparticles. The reported formulations had mean particle sizes below 200 nm, relatively narrow particle-size distributions, positive surface charges, and substantial alkaloid incorporation. Among the single-drug formulations, berberine-loaded nanoparticles had the highest reported encapsulation efficiency. Compared with free berberine, the nanoencapsulated formulation showed slower cumulative release and lower MCF-7 metabolic viability across the tested concentration range. These findings indicate that polymeric encapsulation modified the in vitro delivery profile of berberine, although they do not establish active tumor targeting, selective cancer-cell toxicity, in vivo efficacy, or clinical safety.

The mean particle sizes of the prepared formulations ranged from 128.6 to 168.5 nm, while the polydispersity index values ranged from 0.214 to 0.269. These findings indicate that the reported formulations were within the nanoscale range and had relatively narrow hydrodynamic size distributions. Particle size and dispersity are important formulation characteristics because they influence colloidal stability, cellular interaction, drug release, systemic clearance, and tissue distribution. However, tumor delivery is determined by a complex interaction between nanoparticle composition, surface chemistry, protein adsorption, circulation time, vascular permeability, tumor perfusion, extracellular-matrix density, and immune clearance. Consequently, nanoscale dimensions alone cannot be interpreted as evidence of tumor-specific delivery (9–11). Wilhelm et al. demonstrated that only a limited proportion of systemically administered nanoparticles typically reaches solid tumors, while Bertrand et al. emphasized that both passive and active targeting remain highly dependent on biological context and formulation properties (9,10).

All formulations showed a positive zeta potential, ranging from +21.4 to +25.6 mV. This finding was consistent with the inclusion of chitosan, a cationic polysaccharide commonly used to modify nanoparticle surfaces. Chitosan-based systems may improve dispersibility, alter adhesion to biological membranes, and influence cellular interaction because positively charged surfaces can interact electrostatically with negatively charged membrane components (15). Nevertheless, the present study did not directly evaluate cellular uptake, membrane binding, intracellular localization, or endocytic pathways. The positive surface charge should therefore be interpreted as a physicochemical property rather than proof of increased cellular internalization.

Berberine-loaded nanoparticles showed an encapsulation efficiency of 82.6 ± 3.4% and drug loading of 14.8 ± 1.2%, while piperine-loaded nanoparticles showed an encapsulation efficiency of 78.4 ± 2.9% and drug loading of 13.2 ± 1.0%. These findings suggest that both alkaloids could be incorporated into the polymeric carrier, with somewhat greater reported incorporation of berberine. Differences in encapsulation may reflect variation in molecular structure, lipophilicity, ionization, drug–polymer affinity, solvent partitioning, and interactions with chitosan and PLGA. Comparable work has shown that berberine can be incorporated into PLGA, liquid-crystalline, gold, and hyaluronic acid-modified nanoparticle systems, with formulation-dependent differences in loading, release, and biological activity (20–25). Piperine has similarly been incorporated into polymeric nanoparticles for experimental breast cancer applications (26,27).

The combined berberine–piperine formulation showed the largest reported particle size and the highest total drug-loading value. However, separate encapsulation efficiencies and loading values for berberine and piperine were not available. The combined value therefore cannot establish whether both compounds were incorporated equally or whether one alkaloid preferentially partitioned into the polymeric matrix. Compound-specific analytical measurements would be required to characterize co-loading efficiency, release synchronicity, and the relative contribution of each alkaloid. Furthermore, the combined formulation was not carried forward into the reported cytotoxicity analysis, preventing assessment of additive, synergistic, or antagonistic effects.

The release findings demonstrated a marked descriptive difference between free berberine and berberine-loaded nanoparticles. At 4 hours, 66.8% of free berberine had been released compared with 34.5% of the nanoencapsulated formulation. At 24 hours, free berberine release exceeded 94%, whereas the nanoparticle formulation had released 76.4% and reportedly continued releasing drug through 48 hours. This pattern is compatible with an initial release of drug located near or adsorbed to the nanoparticle surface, followed by slower diffusion from the polymeric matrix and progressive polymer-associated release. Drug liberation from PLGA systems may involve diffusion, matrix relaxation, pore formation, and polymer erosion, depending on polymer composition and formulation conditions (13,14).

The observed release pattern is broadly consistent with the theoretical principles described by Higuchi and Korsmeyer and Peppas (34,35). Nevertheless, the available manuscript did not provide complete time-point data, measures of variability, kinetic coefficients, release exponents, or goodness-of-fit estimates. It was therefore not possible to determine whether the release process was best explained by zero-order, first-order, Higuchi, Korsmeyer–Peppas, or mixed kinetics. A complete kinetic analysis should include all sampling points, replicate-level values, model parameters, and an objective comparison of model fit.

The MCF-7 assay showed a concentration-dependent reduction in metabolic viability following exposure to both free and nanoencapsulated berberine. At 12.5 μg/mL, viability was 84.6 ± 3.5% with free berberine and 76.3 ± 3.2% with berberine-loaded nanoparticles. The difference widened as concentration increased, reaching 16.9 percentage points at 50 μg/mL and 18.2 percentage points at 100 μg/mL. The relative reduction in viability associated with the nanoencapsulated formulation increased from 9.8% at 12.5 μg/mL to 45.8% at 100 μg/mL. These descriptive findings suggest that nanoencapsulation was associated with a greater reduction in MCF-7 metabolic activity at equivalent nominal concentrations.

The reported IC_{50} was 56.4 μg/mL for free berberine and 38.7 μg/mL for berberine-loaded nanoparticles, representing a 17.7 μg/mL absolute difference and an approximately 31.4% lower point estimate for the nanoencapsulated formulation. Similar studies have reported increased cytotoxic effects after berberine incorporation into nanocarriers. Berberine-loaded gold nanoparticles promoted apoptosis-related effects in breast cancer models, while liquid-crystalline and PLGA-based formulations improved berberine delivery and experimental anticancer activity (20–23). Hyaluronic acid-grafted PLGA nanoparticles have also been studied as sustained-delivery systems for berberine in tumor models (25). These comparisons support the general feasibility of nanoformulation but do not establish equivalence between delivery systems because polymer composition, particle characteristics, exposure duration, dose expression, cell line, and assay design differ substantially across studies.

The stronger reduction in metabolic viability observed with the nanoparticle formulation may have resulted from several possible factors, including improved aqueous dispersion, prolonged extracellular availability, increased association with the cell membrane, enhanced intracellular exposure, or gradual drug release. However, none of these mechanisms was directly measured in the present experiment. Cellular-uptake assays, fluorescence or mass-spectrometric quantification, intracellular localization studies, apoptosis assays, cell-cycle analysis, mitochondrial assessments, and mechanistic signaling experiments would be required to determine how the nanoformulation produced its observed effect.

Blank nanoparticles maintained MCF-7 viability above 91% across the tested concentration range. This finding indicates limited carrier-associated reduction in metabolic viability under the specific 48-hour assay conditions. It should not be interpreted as evidence that the carrier was universally safe, biocompatible, or non-toxic. The study did not include non-malignant breast epithelial cells, primary cells, immune-cell models, hemocompatibility testing, organ-toxicity assessment, or animal experiments. The absence of a non-malignant comparator also prevented calculation of a selectivity index and made it impossible to determine whether the formulation preferentially affected malignant rather than normal cells.

The interpretation of the cytotoxicity findings is further limited by the nature of the MTT assay. MTT reduction reflects metabolic activity and does not distinguish between temporary metabolic suppression, reduced proliferation, apoptosis, necrosis, or other forms of cell injury (36). Nanoparticles may also interfere with colorimetric assays through optical absorption, scattering, adsorption of assay reagents, or retention of formazan. Appropriate cell-free nanoparticle controls and background correction are therefore essential. Confirmation using complementary viability and cell-death assays would strengthen the biological interpretation.

This study had several strengths. It evaluated multiple alkaloid-containing formulations, incorporated both physicochemical and biological endpoints, compared free drug with nanoencapsulated drug, included blank nanoparticles, and examined concentration-dependent effects. The integrated assessment of particle size, surface charge, loading, release, and MCF-7 viability provided a useful preliminary framework for evaluating polymeric alkaloid formulations.

The study also had important limitations. The available report did not provide complete formulation compositions, manufacturing parameters, reagent specifications, analytical validation, instrument settings, independent batch numbers, complete release data, or detailed cell-culture quality-control information. The replication structure was unclear, and technical replicates were not distinguished from independently prepared batches or biological experiments. Inferential statistical outputs, confidence intervals, post hoc comparisons, kinetic-model coefficients, and nonlinear dose–response parameters were not supplied. The identity of the alkaloid used in the MTT assay was not stated consistently and was inferred to be berberine from the surrounding manuscript. Morphological examination was described, but scanning electron micrographs were not presented. The combined berberine–piperine formulation was not evaluated biologically, and no non-malignant cell line, cellular-uptake assay, apoptosis assessment, or in vivo model was included.

A further fundamental concern is that the original table titles identified the numerical findings as "example data." All values must therefore be verified against original formulation sheets, instrument exports, analytical files, plate-reader data, and statistical outputs before they can be treated as authentic experimental findings. If the values are illustrative or simulated rather than experimentally generated, they cannot support an original research article.

Subject to verification of the source data, the findings support further investigation of PLGA–chitosan nanoparticles as carriers for poorly bioavailable herbal alkaloids. Future work should establish compound-specific loading in combined formulations, perform validated release-kinetic modelling, include authenticated non-malignant and malignant cell lines, assess cellular uptake and mechanisms of cell death, calculate selectivity indices, evaluate long-term formulation stability, and proceed to pharmacokinetic and animal tumor studies only after robust in vitro confirmation. Such investigations would be required before claims concerning tumor targeting, therapeutic efficacy, or clinical applicability could be justified.

CONCLUSION

PLGA–chitosan nanoparticles successfully incorporated berberine and piperine and showed nanoscale particle dimensions, positive surface charge, and substantial reported drug loading. Berberine-loaded nanoparticles demonstrated slower in vitro release than free berberine and produced lower MCF-7 metabolic viability across the tested concentration range, with a lower reported IC_{50} point estimate. These findings suggest that nanoencapsulation modified berberine release and cytotoxicity under the tested laboratory conditions; however, they do not demonstrate tumor-specific targeting, selective toxicity, in vivo safety, or therapeutic efficacy. Verification of the original experimental data and further mechanistic and preclinical investigation are required.

REFERENCES

1. Sung H, Ferlay J, Siegel RL, Laversanne M, Soerjomataram I, Jemal A, et al. Global cancer statistics 2020: GLOBOCAN estimates of incidence and mortality worldwide for 36 cancers in 185 countries. CA Cancer J Clin. 2021;71(3):209–49. doi:10.3322/caac.21660.

2. Ferlay J, Colombet M, Soerjomataram I, Parkin DM, Piñeros M, Znaor A, et al. Cancer statistics for the year 2020: an overview. Int J Cancer. 2021;149(4):778–89. doi:10.1002/ijc.33588.

3. Ikram A, Pervez S, Khadim MT, Sohaib M, Uddin H, Badar F, et al. National Cancer Registry of Pakistan: first comprehensive report of cancer statistics 2015–2019. J Coll Physicians Surg Pak. 2023;33(6):857–64. doi:10.29271/jcpsp.2023.06.857.

4. Badar F, Mahmood S. Cancer in Lahore, Pakistan, 2010–2019: an incidence study. BMJ Open. 2021;11(8):e047049. doi:10.1136/bmjopen-2020-047049.

5. Pervez S, Jabbar AA, Haider G, Ashraf S, Qureshi MA, Lateef F, et al. Karachi Cancer Registry: age-standardized incidence rate by age-group and gender in a mega city of Pakistan. Asian Pac J Cancer Prev. 2020;21(11):3251–8. doi:10.31557/APJCP.2020.21.11.3251.

6. Pervez S, Jabbar AA, Haider G, Qureshi MA, Ashraf S, Lateef F, et al. Karachi Cancer Registry: consolidated data of 5 years, 2017–2021. J Coll Physicians Surg Pak. 2023;33(5):560–5. doi:10.29271/jcpsp.2023.05.560.

7. Shi J, Kantoff PW, Wooster R, Farokhzad OC. Cancer nanomedicine: progress, challenges and opportunities. Nat Rev Cancer. 2017;17(1):20–37. doi:10.1038/nrc.2016.108.

8. Rosenblum D, Joshi N, Tao W, Karp JM, Peer D. Progress and challenges towards targeted delivery of cancer therapeutics. Nat Commun. 2018;9:1410. doi:10.1038/s41467-018-03705-y.

9. Wilhelm S, Tavares AJ, Dai Q, Ohta S, Audet J, Dvorak HF, et al. Analysis of nanoparticle delivery to tumours. Nat Rev Mater. 2016;1:16014. doi:10.1038/natrevmats.2016.14.

10. Bertrand N, Wu J, Xu X, Kamaly N, Farokhzad OC. Cancer nanotechnology: the impact of passive and active targeting in the era of modern cancer biology. Adv Drug Deliv Rev. 2014;66:2–25. doi:10.1016/j.addr.2013.11.009.

11. Mitchell MJ, Billingsley MM, Haley RM, Wechsler ME, Peppas NA, Langer R. Engineering precision nanoparticles for drug delivery. Nat Rev Drug Discov. 2021;20(2):101–24. doi:10.1038/s41573-020-0090-8.

12. Yao Y, Zhou Y, Liu L, Xu Y, Chen Q, Wang Y, et al. Nanoparticle-based drug delivery in cancer therapy and its role in overcoming drug resistance. Front Mol Biosci. 2020;7:193. doi:10.3389/fmolb.2020.00193.

13. Patra JK, Das G, Fraceto LF, Campos EVR, Rodriguez-Torres MP, Acosta-Torres LS, et al. Nano based drug delivery systems: recent developments and future prospects. J Nanobiotechnology. 2018;16:71. doi:10.1186/s12951-018-0392-8.

14. Afzal O, Altamimi ASA, Nadeem MS, Alzarea SI, Almalki WH, Tariq A, et al. Nanoparticles in drug delivery: from history to therapeutic applications. Nanomaterials (Basel). 2022;12(24):4494. doi:10.3390/nano12244494.

15. Mikušová V, Mikuš P. Advances in chitosan-based nanoparticles for drug delivery. Int J Mol Sci. 2021;22(17):9652. doi:10.3390/ijms22179652.

16. Chavda VP, Vora LK, Pandya AK, Patravale VB. Nano-drug delivery systems entrapping natural bioactive compounds for cancer: recent progress and future challenges. Front Oncol. 2022;12:867655. doi:10.3389/fonc.2022.867655.

17. Li B, Shao H, Gao L, Li H, Sheng H, Zhu L. Nano-drug co-delivery system of natural active ingredients and chemotherapy drugs for cancer treatment: a review. Drug Deliv. 2022;29(1):2130–61. doi:10.1080/10717544.2022.2094498.

18. Xiong RG, Huang SY, Wu SX, Zhou DD, Yang ZJ, Saimaiti A, et al. Anticancer effects and mechanisms of berberine from medicinal herbs: an update review. Molecules. 2022;27(14):4523. doi:10.3390/molecules27144523.

19. Zhu Y, Xie N, Chai Y, Nie Y, Liu K, Liu Y, et al. Apoptosis induction, a sharp edge of berberine to exert anti-cancer effects, focus on breast, lung, and liver cancer. Front Pharmacol. 2022;13:803717. doi:10.3389/fphar.2022.803717.

20. Khan I, Joshi G, Nakhate KT, Ajazuddin, Kumar R, Gupta U. Nano-co-delivery of berberine and anticancer drug using PLGA nanoparticles: exploration of better anticancer activity and in vivo kinetics. Pharm Res. 2019;36(10):149. doi:10.1007/s11095-019-2677-5.

21. Chiu CF, Fu RH, Hsu SH, Yu YH, Yang SF, Tsao TCY, et al. Delivery capacity and anticancer ability of the berberine-loaded gold nanoparticles to promote the apoptosis effect in breast cancer. Cancers (Basel). 2021;13(21):5317. doi:10.3390/cancers13215317.

22. Loo YS, Madheswaran T, Rajendran R, Bose RJC. Encapsulation of berberine into liquid crystalline nanoparticles to enhance its solubility and anticancer activity in MCF7 human breast cancer cells. J Drug Deliv Sci Technol. 2020;57:101756. doi:10.1016/j.jddst.2020.101756.

23. Paudel KR, Mehta M, Yin GHS, Yen LL, Malyla V, Patel VK, et al. Berberine-loaded liquid crystalline nanoparticles inhibit non-small cell lung cancer proliferation and migration in vitro. Environ Sci Pollut Res Int. 2022;29(31):46830–47. doi:10.1007/s11356-022-19158-2.

24. Farahani M, Moradikhah F, Shabani I, Soflou RK, Seyedjafari E. Microfluidic fabrication of berberine-loaded nanoparticles for cancer treatment applications. J Drug Deliv Sci Technol. 2021;61:102134. doi:10.1016/j.jddst.2020.102134.

25. Bhatnagar P, Kumari M, Pahuja R, Pant AB, Shukla Y, Kumar P, et al. Hyaluronic acid-grafted PLGA nanoparticles for the sustained delivery of berberine chloride for an efficient suppression of Ehrlich ascites tumors. Drug Deliv Transl Res. 2018;8(3):565–79. doi:10.1007/s13346-018-0485-9.

26. Kazmi I, Al-Abbasi FA, Imam SS, Afzal M, Nadeem MS, Altayb HN, et al. Formulation of piperine nanoparticles: in vitro breast cancer cell line and in vivo evaluation. Polymers (Basel). 2022;14(7):1349. doi:10.3390/polym14071349.

27. Gilani SJ, Bin-Jumah MN, Fatima F. Development of statistically optimized piperine-loaded polymeric nanoparticles for breast cancer: in vitro evaluation and cell culture studies. ACS Omega. 2023;8:44183–94. doi:10.1021/acsomega.3c06605.

28. Martino E, Della Volpe S, Terribile E, Benetti E, Sakaj M, Centamore A, et al. The long story of camptothecin: from traditional medicine to drugs. Bioorg Med Chem Lett. 2017;27(4):701–7. doi:10.1016/j.bmcl.2016.12.085.

29. Wen Y, Wang Y, Liu X, Zhang W, Xiong X, Han Z, et al. Camptothecin-based nanodrug delivery systems. Cancer Biol Med. 2017;14(4):363–70. doi:10.20892/j.issn.2095-3941.2017.0099.

30. Ghanbari-Movahed M, Kaceli T, Mondal A, Farzaei MH, Bishayee A. Recent advances in improved anticancer efficacies of camptothecin nano-formulations: a systematic review. Biomedicines. 2021;9(5):480. doi:10.3390/biomedicines9050480.

31. Ullah A, Munir S, Badshah SL, Khan N, Ghani L, Poulson BG, et al. Molecular mechanisms of sanguinarine in cancer prevention and treatment. Anticancer Agents Med Chem. 2023;23(7):765–78. doi:10.2174/1871520622666220831124321.

32. Solanki R, Tandel H, Patel P, Patel D, Patel J, Patel M, et al. Enhancing apoptosis-mediated anticancer activity of evodiamine in biodegradable polymeric nanoparticles. Sci Rep. 2024;14:2595. doi:10.1038/s41598-024-51970-3.

33. Zou L, Liu X, Cao Y, Zheng Y, Zhang Y, Zhang T, et al. Preparation, characterization, and anticancer efficacy of evodiamine-loaded solid lipid nanoparticles. Drug Deliv. 2016;23(7):2324–33. doi:10.3109/10717544.2014.920936.

34. Higuchi T. Mechanism of sustained-action medication: theoretical analysis of rate of release of solid drugs dispersed in solid matrices. J Pharm Sci. 1963;52(12):1145–9. doi:10.1002/jps.2600521210.

35. Korsmeyer RW, Gurny R, Doelker E, Buri P, Peppas NA. Mechanisms of solute release from porous hydrophilic polymers. Int J Pharm. 1983;15(1):25–35. doi:10.1016/0378-5173(83)90064-9.

36. Mosmann T. Rapid colorimetric assay for cellular growth and survival: application to proliferation and cytotoxicity assays. J Immunol Methods. 1983;65(1–2):55–63. doi:10.1016/0022-1759(83)90303-4.